Subdivision schemes for shape preserving approximations

Francesca Pitolli
Dept. SBAI, Università di Roma "La Sapienza"
Via Antonio Scarpa, 00161 Roma, Italy
francesca.pitolli@sbai.uniroma1.it

Abstract

We use subdivision schemes with general dilation to efficiently evaluate shape preserving approximations. To fulfill our goal the refinement rules of the schemes are obtained by the refinement masks associated to refinable ripplets, i.e. refinable functions whose integer translates form a variation diminishing basis.

Keywords: Shape-preserving, Variation diminishing, Ripplet, Refinable function, Subdivision scheme

1. Introduction

Shape preserving approximations are used in the design of curves or surfaces to *predict or control their 'shape'* by the shape of the *control points*, i.e. the vertices of a given polygonal arc or polyhedral surface. Shape preserving approximations have applications, for instance, in Computer Aided Design, in Computer Graphics and in the Design of Fonts (see [6, 13] for a survey on the topic). On the other hand, in Approximation Theory the construction of approximation operators that *mimic the 'shape'*, i.e. reproduce the monotonicity and/or the convexity, of the function to be approximated is required in many applications (see [7] and references therein). The key ingredient to construct shape preserving approximations and operators is the *variation diminishing property*.
Let $\mathcal{U} = \{u_i(x)\,, i \in Z\}$, $Z \subseteq \mathbb{Z}$, $x \in I \subseteq \mathbb{R}$, denote a function basis of a given space

$$\mathcal{V} = \Big\{v : v(x) = \sum_{i\in Z} q_i\, u_i(x)\,,\ x \in I\,,\ q_i \in \mathbb{R}\Big\}\,. \tag{1}$$

The basis $\mathcal{U}$ is variation diminishing if for any sequence $\mathbf{q} = \{q_i \in \mathbb{R}\,, i \in Z\}$,

$$S^-\big(\sum_{i\in Z} q_i\, u_i(x)\big) \le S^-(\mathbf{q})\,, \qquad x \in I\,, \tag{2}$$

where S^- denotes the strict sign changes in its argument ([14, 15]).
When $\mathcal{U}$ is a variation diminishing and *normalized basis*, i.e. $\mathcal{U}$ satisfies (2) and

$$\sum_{i \in Z} u_i(x) = 1\,, \qquad x \in I\,, \tag{3}$$

then the numbers of times the curve

$$\gamma(x) = \sum_{i \in Z} \mathbf{P}_i\, u_i(x)\,, \qquad \mathbf{P}_i \in \mathbb{R}^2\,, \qquad x \in I\,, \tag{4}$$

crosses any straight line L is bounded by the number of times the control polygon $\mathbf{\Pi} = \{\mathbf{P}_i, i \in \mathbb{Z}\}$ crosses L. As a consequence, if the control polygon $\mathbf{\Pi}$ is monotonic in a given direction, then so is the curve γ. Moreover, assume u_i are continuous; if the control polygon $\mathbf{\Pi}$ is convex, then so is the curve γ. Thus, we say that γ is a *shape preserving representation* of $\mathbf{\Pi}$ [7, 15].
Now, let us assume that the monomial x can be represented by the basis $\mathcal{U}$, i.e. there exists a strictly increasing sequence of *real numbers* $\{\xi_i,\, i \in Z\}$, such that

$$x = \sum_{i \in Z} \xi_i\, u_i(x)\,, \qquad x \in I\,. \tag{5}$$

Then, the linear operator

$$(\mathcal{S}f)(x) = \sum_{i \in Z} f(\xi_i)\, u_i(x)\,, \qquad x \in I\,, \tag{6}$$

preserves the monotonicity and the convexity of f, i.e. $\mathcal{S}f$ is a *shape preserving approximating operator* [7].

In applications both the curve γ and the operator $\mathcal{S}f$ need to be evaluated *efficiently*. Our goal is to construct efficient algorithms for the generation of shape preserving approximations.

The paper is as follows. In Section 2 we will describe some efficient shape preserving algorithms to evaluate spline curves and we will show a strategy to construct more general algorithms for the generation of shape preserving approximations. In Section 3 we will introduce a wide family of algorithms and analyze their properties and performances.

2. Refinable Ripplets and Subdivision Schemes

Well known examples of variation diminishing bases on $\mathbb{R}$ are the cardinal B-splines, i.e. piecewise polynomial on integer knots (see the monographs [14, 15, 16] for basic definitions and main properties of B-splines).
Let B_N denote the B-spline of degree N with $N+2$ integer knots on $[0, N+1]$. The basis $\mathcal{B}_N = \{B_N(x-k), k \in \mathbb{Z}\}$, $x \in \mathbb{R}$, is variation diminishing ([14]) so that the spline curve

$$\gamma_N(x) = \sum_{k \in \mathbb{Z}} \mathbf{P}_k\, B_N(x-k)\,, \qquad x \in \mathbb{R}\,, \qquad \mathbf{P}_k \in \mathbb{R}^2\,, \tag{7}$$

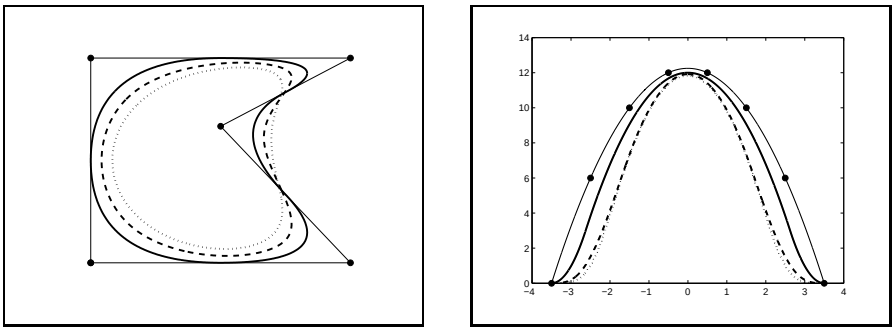

Figure 1: The spline curve γ_N representing the control polygon $\mathbf{\Pi_c}$ (left) and the operator $\mathcal{S}_N f$ with f as in (10) (right) for $N = 2$ (solid line), $N = 3$ (dashed line) and $N = 4$ (dotted line) . The control polygon (thin line), the control points (circles), the function f (thin line) and the the points $(\xi_k, f(\xi_k))$ (circles) with $\xi_k = k + (N+1)/2 \in [-3.5, 3.5]$ are also displayed.

is a shape preserving representation of the control polygon $\mathbf{\Pi}$. Moreover, since for $N \geq 1$ ([16])

$$x = \sum_{k\in\mathbb{Z}} \left(k + \tfrac{N+1}{2}\right) B_N(x-k)\,, \qquad x \in \mathbb{R}\,, \tag{8}$$

the operator

$$(\mathcal{S}_N f)(x) = \sum_{i\in Z} f\left(k + \tfrac{N+1}{2}\right) B_N(x-k)\,, \qquad x \in \mathbb{R}\,, \qquad N \geq 1\,, \tag{9}$$

is shape preserving ([7]).

In Fig. 1 (left) some spline curves γ_N representing the closed control polygon $\mathbf{\Pi}_c = \mathbf{P}_1\mathbf{P}_2\mathbf{P}_3\mathbf{P}_4\mathbf{P}_5\mathbf{P}_6$ with $\mathbf{P}_1 \equiv \mathbf{P}_6 = (0,0)$, $\mathbf{P}_2 = (1,0)$, $\mathbf{P}_3 = (\frac{1}{2}, \frac{2}{3})$, $\mathbf{P}_4 = (1,1)$, $\mathbf{P}_5 = (0,1)$, are shown. Here periodic conditions for closed curves have been used. In Fig. 1 (right) the operator $\mathcal{S}_N f$ when f is the function

$$f(x) = \begin{cases} (-3.5 - x)(-3.5 + x)\,, & -3.5 \leq x \leq 3.5\,, \\ 0\,, & \text{otherwise}\,, \end{cases} \tag{10}$$

is displayed for $N = 2, 3, 4$. We note that in case of closed interval suitable boundary functions at the end points have to be used ([16]).

In order to evaluate efficiently the curve γ_N or the operator $\mathcal{S}_N f$ suitable algorithms are needed. For instance, the Chaikin's algorithm [2]

$$\mathbf{P}^m_{2k} = \frac{3}{4}\,\mathbf{P}^{m-1}_k + \frac{1}{4}\,\mathbf{P}^{m-1}_{k+1}\,, \quad \mathbf{P}^m_{2k+1} = \frac{1}{4}\,\mathbf{P}^{m-1}_k + \frac{3}{4}\,\mathbf{P}^{m-1}_{k+1}\,, \qquad m \geq 1\,, \tag{11}$$

is an efficient algorithm to generate quadratic spline curves starting from a set of control points $\{\mathbf{P}^0_k\}$. Chaikin's algorithm is a simple example of a wide class of algorithms, usually called *corner cutting algorithms*. The algorithm *cuts*

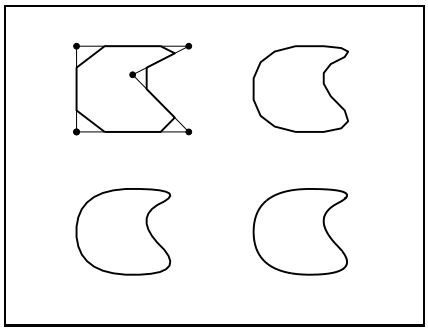

Figure 2: The first three iterations of the Chaikin's algorithm (top-left, top-right, bottom-left) and the limit quadratic spline curve (bottom-right) for the control polygon $\mathbf{\Pi}_c$. The starting control points are displayed as circles.

iteratively the corners of the polygonal arc $\{\mathbf{P}_k^{m-1}, k \in \mathbb{Z}\}$ converging in the limit to a smooth curve (see [15] and references therein for details). In Fig. 2 the first three iterations of the Chaikin's algorithm and the limit quadratic spline curve are displayed.

Chaikin's algorithm is closely related to the property of the quadratic cardinal B-spline to be a *refinable functions*. In fact, for any $N \geq 0$ the cardinal B-spline B_N satisfies the refinement equation

$$B_N(x) = \sum_{k=0}^{(M-1)(N+1)} b_{k,N,M}\, B_N(Mx-k)\,, \qquad x \in \mathbb{R}\,, \tag{12}$$

where the *dilation* $M \geq 2$ is an integer and the sequence $\mathbf{b}_{N,M} = \{b_{k,N,M}, 0 \leq k \leq (M-1)(N+1)\}$ is the *refinement mask* ([3, 4]). For any N and M held fixed, the explicit expression of the mask coefficients $b_{k,N,M}$, $0 \leq k \leq (M-1)(N+1)$, can be obtained by the equality

$$\sum_{k=0}^{(M-1)(N+1)} b_{k,N,M}\, z^k = \frac{1}{M^N}\big(1 + z + z^2 + \cdots + z^{M-1}\big)^{N+1}\,. \tag{13}$$

For $N = 2$ and $M = 2$ the mask coefficients $b_{0,2,2} = b_{3,2,2} = \frac{1}{4}$ and $b_{1,2,2} = b_{2,2,2} = \frac{3}{4}$, are the same coefficients as those in the Chaikin's algorithm (11). More in general, any refinement mask $\mathbf{b}_{N,M}$ gives rise to the *subdivision algorithm*

$$\begin{cases} \mathbf{P}_k^0 = \mathbf{P}_k \in \mathbb{R}^2\,, \quad k \in \mathbb{Z}\,, \\ \\ \mathbf{P}_j^m = \sum_{k\in\mathbb{Z}} b_{j-Mk,N,M}\, \mathbf{P}_k^{m-1}\,, \qquad j \in \mathbb{Z}\,, \qquad m \geq 1\,, \end{cases} \tag{14}$$

(see [1, 5] for a complete treatment of the topic). Starting from the initial set of points $\{\mathbf{P}_k^0\}$ attached to the regular grid $M\mathbb{Z}$, the algorithm generates denser

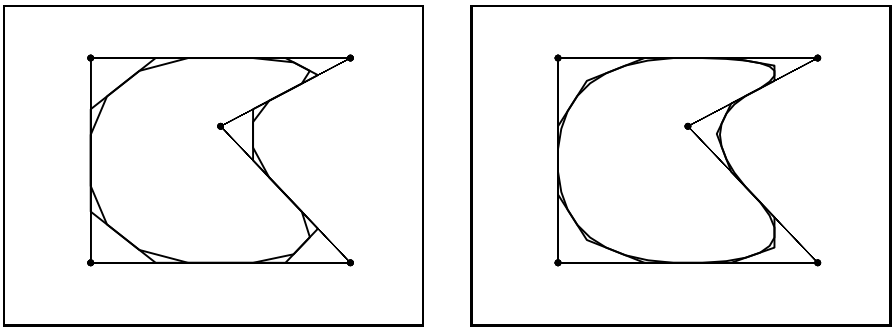

Figure 3: The first two iterations of the Chaikin's algorithm (11) (left) and of the subdivision scheme (17) (right). The control polygon (thin line) and the control points (circles) are also displayed.

sequences of points parametrized so that the points $\mathbf{P}_k^m$ correspond to the finer grid $M^{-m}\mathbb{Z}$. In the limit the denser point sequences converge to the N-degree spline curve γ_N representing the polygon $\{\mathbf{P}_k^0, k \in \mathbb{Z}\}$. In particular, for $M = 2$ we have a dyadic refinement with refinement mask $\mathbf{b}_{N,2} = \{b_{k,N,2}\}$ given by ([3])

$$b_{k,N,2} = \frac{1}{2^N} \binom{N+1}{k}, \qquad 0 \le k \le N+1\,, \tag{15}$$

while for $M = 3$ we have a ternary refinement with refinement mask $\mathbf{b}_{N,3} = \{b_{k,N,3}\}$ ([12])

$$b_{k,N,3} = \frac{1}{3^N} \sum_{j=[(k+1)/2]}^{k} \binom{N+1}{j} \binom{j}{k-j}, \qquad 0 \le k \le 2(N+1)\,. \tag{16}$$

In particular, the explicit expression of the subdivision algorithm associated with the refinement mask $\mathbf{b}_{2,3}$ is given by

$$\begin{cases} \mathbf{P}_{3k}^m = \frac{1}{9}\,\mathbf{P}_k^{m-1} + \frac{7}{9}\,\mathbf{P}_{k+1}^{m-1} + \frac{1}{9}\,\mathbf{P}_{k+2}^{m-1}\,, \\ \mathbf{P}_{3k+1}^m = \frac{1}{3}\,\mathbf{P}_k^{m-1} + \frac{2}{3}\,\mathbf{P}_{k+1}^{m-1}\,, \qquad\qquad m \ge 1\,. \\ \mathbf{P}_{3k+2}^m = \frac{2}{3}\,\mathbf{P}_k^{m-1} + \frac{1}{3}\,\mathbf{P}_{k+1}^{m-1}\,, \end{cases} \tag{17}$$

As the Chaikin's algorithm, the algorithm above converges to the quadratic spline curve representing the control polygon $\mathbf{\Pi} = \{\mathbf{P}_k^0, k \in \mathbb{Z}\}$ but the convergence is faster since at any iteration the points are multiplied by three. This can be seen in Fig. 3 where the first two iterations of the Chaikin's algorithm and the subdivision scheme (17) are displayed.

The B-spline example suggests us a strategy to construct efficient algorithms giving rise to shape preserving approximations. First of all, we note that the variation diminishing property of the cardinal B-spline basis $\mathcal{B}_N$ relies on the property of B_N to be a ripplet.

We recall that a function u is said to be a *ripplet* if for any strictly increasing sequence $\{x_i \in \mathbb{R}, 1 \le i \le p\}$ all the minors of the collocation matrix $(u(x_i - k), k \in \mathbb{Z},\ 1 \le i \le p)$ are non negative [8].

Thus, the first step to construct efficient shape preserving algorithms is the construction of *refinable ripplets*, i.e. ripplets satisfying the refinement equation

$$\varphi_{\mathbf{a}}(x) = \sum_{k=0}^{(M-1)(N+1)} a_k \, \varphi_{\mathbf{a}}(Mx - k)\,, \qquad x \in \mathbb{R}\,, \tag{18}$$

where the sequence $\mathbf{a} = \{a_k \in \mathbb{R}, 0 \le k \le (M-1)(N+1)\}$ is the refinement mask. Conditions on the mask coefficients ensuring that $\varphi_{\mathbf{a}}$ is a ripplet was given in [8] for dilation $M = 2$ and in [9] for dilation $M \ge 3$.

Since $\varphi_{\mathbf{a}}$ is a ripplet, the basis $\Phi_{\mathbf{a}} = \{\varphi_{\mathbf{a}}(x - k), k \in \mathbb{Z}\}$, $x \in \mathbb{R}$, enjoys the variation diminishing property and the curve

$$\gamma_{\mathbf{a}}(x) = \sum_{k \in \mathbb{Z}} \mathbf{P}_k \, \varphi_{\mathbf{a}}(x - k)\,, \qquad \mathbf{P}_i \in \mathbb{R}^2\,, \qquad x \in \mathbb{R}\,, \tag{19}$$

preserves the shape of the control polygon $\mathbf{\Pi} = \{\mathbf{P}_k, k \in \mathbb{Z}\}$.

On the other hand, when $\varphi_{\mathbf{a}}$ is refinable, the refinement mask $\mathbf{a}$ can be used in a subdivision algorithm to evaluate efficiently the curve $\gamma_{\mathbf{a}}$. In fact, when $\varphi_{\mathbf{a}}$ is a ripplet the algorithm

$$\begin{cases} \mathbf{P}_k^0 = \mathbf{P}_k \in \mathbb{R}^2\,, & k \in \mathbb{Z}\,, \\ \mathbf{P}_j^m = \sum_{k \in \mathbb{Z}} a_{j-Mk} \, \mathbf{P}_k^{m-1}\,, & j \in \mathbb{Z}\,, \qquad m \ge 1\,, \end{cases} \tag{20}$$

converges to $\gamma_{\mathbf{a}}$ [1, 8, 9].
Moreover, if there exist *real numbers* ξ_k, $k \in \mathbb{Z}$, such that

$$x = \sum_{k \in \mathbb{Z}} \xi_k \, \varphi_{\mathbf{a}}(x - k)\,, \qquad x \in \mathbb{R}\,, \quad \xi_k < \xi_{k+1}\,, \tag{21}$$

then the linear operator

$$(\mathcal{S}_{\mathbf{a}} f)(x) = \sum_{k \in \mathbb{Z}} f(\xi_k) \, \varphi_{\mathbf{a}}(x - k)\,, \qquad x \in \mathbb{R}\,, \tag{22}$$

is a shape preserving representation of the function f and the subdivision algorithm

$$\begin{cases} f_k^0 = f(\xi_k)\,, & k \in \mathbb{Z}\,, \\ f_k^m = \sum_{k \in \mathbb{Z}} a_{j-Mk} \, f_j^{m-1}\,, & j \in \mathbb{Z}\,, \qquad m \ge 1\,, \end{cases} \tag{23}$$

converges to $\mathcal{S}_{\mathbf{a}} f$ [5, 8, 9].

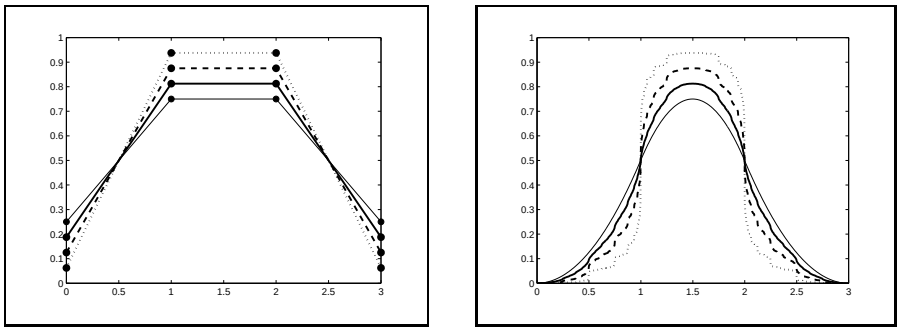

Figure 4: Left: The coefficients of the refinement mask $\mathbf{a}_{h,2,2}$ (circles) for $h = 0.75$ (solid line), $h = 0.5$ (dashed line) and $h = 0.25$ (dotted line). Right: The C^0-refinable function $\varphi_{h,2,2}$ for $h = 0.75$ (solid line), $h = 0.5$ (dashed line) and $h = 0.25$ (dotted line). For comparison, the mask $\mathbf{a}_{1,2,2} \equiv \mathbf{b}_{2,2}$ and $\varphi_{1,2,2} \equiv B_2$ are also displayed (thin line).

3. Classes of shape preserving subdivision schemes

Wide classes of refinable ripplets with dilation $M = 2, 3$ were constructed in [10, 12]. They are solution to the refinement equation

$$\varphi_{h,N,M}(x) = \sum_{k=0}^{(M-1)(N+1)} a_{k,h,N,M}\, \varphi_{h,N,M}(Mx - k)\,, \qquad x \in \mathbb{R}\,, \tag{24}$$

where any refinement mask $\mathbf{a}_{h,N,M} = \{a_{k,h,N,M} \in \mathbb{R}, 0 \le k \le (M-1)(N+1)\}$ is a positive, bell-shaped, centrally symmetric sequence. For any $N \ge 2$ and $M = 2, 3$, the explicit expression of the mask coefficients is given by

$$a_{k,h,N,M} = h\, b_{k,N,M} + (1-h)\, b_{k-1,M+N-4,M}\,, \tag{25}$$

where $0 \le h \le 1$ is a *real parameter* and $b_{r,N,M} = 0$ for $r < 0$ and $r > (M-1)(N+1)$.
The parameter h acts as a *shape parameter* that controls the shape of the refinable ripplet $\varphi_{h,N,M}$ through the values of the mask coefficients. The relation between the behavior of the mask coefficients and the shape of the corresponding refinable function is put in evidence in Fig. 4 and Fig. 5 where the graphs of $\varphi_{h,2,2}$ and $\varphi_{h,2,3}$ for different values of h are displayed. We note that both $\varphi_{h,2,2}$ and $\varphi_{h,2,3}$ have compact support $[0, 3]$ but $\varphi_{h,2,2}$ is just C^0 while $\varphi_{h,2,3}$ belongs to C^1.

The properties of $\varphi_{h,N,M}$ are related to the properties of the refinement mask $\mathbf{a}_{h,N,M}$. In particular, since any mask (25) is compactly supported, positive, centrally symmetric and bell-shaped any refinable ripplets $\varphi_{h,N,M}$ is compactly supported with $supp\, \varphi_{h,N,M} = [0, N+1]$, positive on $(0, N+1)$, centrally symmetric and bell-shaped. Moreover, $\varphi_{h,N,M} \in C^{N+M-4}$ (see [10, 12] for details).

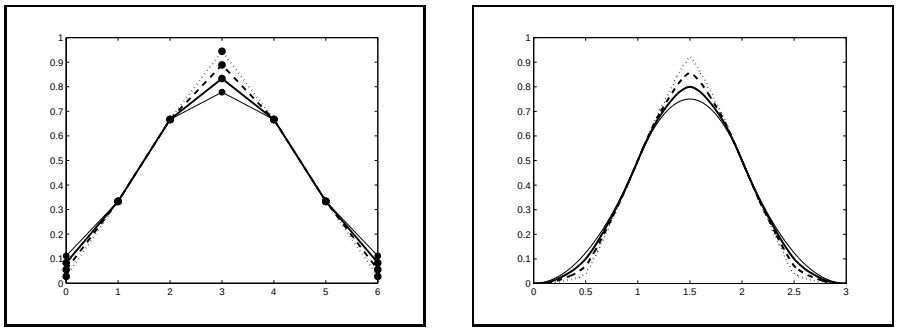

Figure 5: Left: The coefficients of the refinement masks $\mathbf{a}_{h,2,3}$ (circles) for $h = 0.75$ (solid line), $h = 0.5$ (dashed line) and 0.25 (dotted line). Right: The C^1-refinable function $\varphi_{h,2,3}$ for $h = 0.75$ (solid line), $h = 0.5$ (dashed line) and $h = 0.25$ (dotted line). For comparison, the mask $\mathbf{a}_{1,2,3} \equiv \mathbf{b}_{2,3}$ and $\varphi_{1,2,3} \equiv B_2$ are also displayed (thin line).

Consider now the function system

$$\Phi_{h,N,M} = \{\varphi_{h,N,M}(x-k)\}_{k\in\mathbb{Z}}\,, \qquad x \in \mathbb{R}\,, \qquad N \geq 2\,, \quad M = 2,3\,.$$

Since $\varphi_{h,N,M}$ is a ripplet, $\Phi_{h,N,M}$ is variation diminishing and the curve

$$\gamma_{\mathbf{a}_{h,N,M}}(x) = \sum_{k\in\mathbb{Z}} \mathbf{P}_k\, \varphi_{h,N,M}(x-k)\,, \qquad \mathbf{P}_k \in \mathbb{R}^2, \quad x \in \mathbb{R}\,, \tag{26}$$

has shape preserving properties. Moreover, for $N \geq 5 - M$ it can be proved that the monomial x can be represented as

$$x = \sum_{k\in\mathbb{Z}} \big(k + \tfrac{N+1}{2}\big)\, \varphi_{h,N,M}(x-k)\,, \qquad x \in \mathbb{R}\,, \tag{27}$$

so that the operator

$$\big(\mathcal{S}_{\mathbf{a}_{h,N,M}} f\big)(x) = \sum_{k\in\mathbb{Z}} f\big(k + \tfrac{N+1}{2}\big)\, \varphi_{h,N,M}(x-k)\,, \qquad x \in \mathbb{R}\,, \tag{28}$$

is shape preserving ([11, 12]).
Both $\gamma_{\mathbf{a}_{h,N,M}}$ and $\mathcal{S}_{\mathbf{a}_{h,N,M}}$ can be evaluated efficiently by a subdivision algorithm similar to that one in (20) and (22), respectively.

Fig. 6 shows how the parameter h affects the shape of the closed curves $\gamma_{h,2,2}$ and $\gamma_{h,2,3}$ when representing the control polygon $\mathbf{\Pi}_c$. We note that for any $h \in (0,1)$ $\gamma_{h,2,2}$ is a C^0-curve that cuts the corner sharply while $\gamma_{h,2,3}$ is a C^1-curve that rounds the corner smoothly. Finally, the graphs in Fig. 7 show the different behavior of the non shape preserving operator $\mathcal{S}_{\mathbf{a}_{h,2,2}} f$ in comparison with the behavior of the shape preserving operator $\mathcal{S}_{\mathbf{a}_{h,2,3}} f$. Here f is as in (10). We note that optimal bases on closed intervals were constructed in [11] for dilation $M = 2$ and in [12] for dilation $M = 3$.

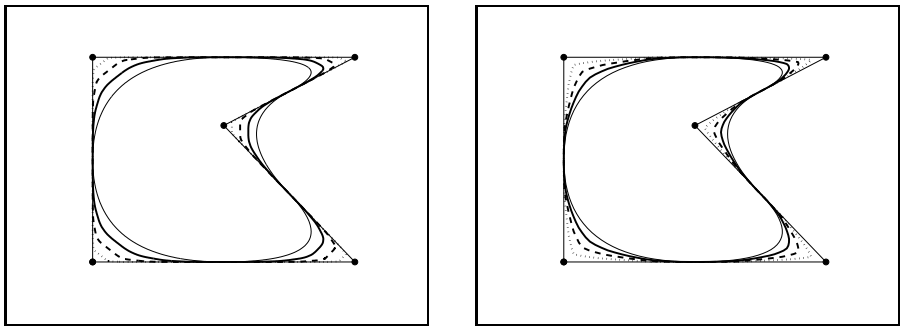

Figure 6: The C^0-curves $\gamma_{h,2,2}$ (left) and the C^1-curves $\gamma_{h,2,3}$ (right) for $h = 0.75$ (solid line), $h = 0.5$ (dashed line) and $h = 0.25$ (dotted line) representing the control polygon $\mathbf{\Pi}_c$. The quadratic B-spline curve is also displayed (thin line).

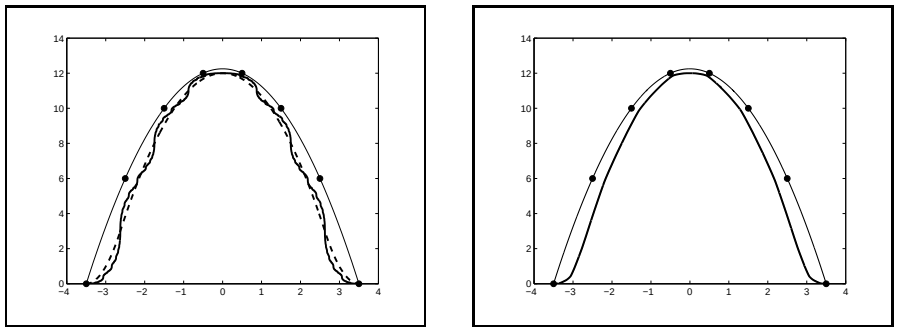

Figure 7: The operators $\mathcal{S}_{h,2,2}f$ (solid line left), $\mathcal{S}_{h,2,3}f$ (solid line right) for $h = 0.5$ and the quadratic B-spline operator (dashed line left). The function f (thin line) and the the points $(\xi_k, f(\xi_k))$ (circles) with $\xi_k = k+3/2 \in [-3.5, 3.5]$ are also displayed.

References

[1] A. Cavaretta, W. Dahmen and C.A. Micchelli, Stationary subdivision, *Mem. Amer. Math. Soc.* **93**, AMS, 1991.

[2] G.M. Chaikin, An algorithm for high-speed curve generation, *Computer Graphics and Image Processing* **3** (1974), 346–349.

[3] C.K. Chui, *An Introduction to Wavelets*, Academic Press, 1992.

[4] C.K. Chui and J.A. Lian, Construction of compactly supported symmetric and antisymmetric orthonormal wavelets with scale 3, *Appl. Comput. Harmon. Anal.* **2** (1995), 21-51.

[5] N. Dyn and D. Levin, Subdivision schemes in geometric modelling, *Acta Numerica* (2002), 1–72.

[6] G. Farin, *Curves and Surfaces for Computer Aided Geometric Design*, Academic Press, 1993.

[7] T.N.T. Goodman, Total positivity and the shape of curves, in *Total positivity and its applications*, 157–186, Kluwer Academic, 1996.

[8] T.N.T. Goodman and C.A. Micchelli, On refinement equations determined by Polya frequency sequences, *SIAM J. Math. Anal.* **23** (1992), 766–784.

[9] T.N.T. Goodman and Q. Sun, Total positivity and refinable functions with general dilation, *Appl. Comput. Harmon. Anal.* **16** (2004), 69–89.

[10] L. Gori L. and F. Pitolli, A class of totally positive refinable functions, *Rend. Mat. Appl.* **20** (2000), 305–322.

[11] L. Gori and F. Pitolli, On some applications of a class of totally positive bases, in *Wavelet Analysis and Applications*, 109–118, American Mathematical Society-International Press, 2002.

[12] L. Gori, F. Pitolli and E. Santi, Refinable ripplets with dilation 3, *Jaen J. Approx.* **3** (2011), 173-191.

[13] J. Hoschek and D. Lasser, *Fundamentals of Computer Aided Geometric Design*, A.K. Peters, 1996.

[14] S. Karlin, *Total Positivity*, Stanford Univ. Press, 1968.

[15] C.A. Micchelli, *Mathematical Aspects of Geometric Modeling*, CBMS-NSF regional conference series in applied mathematics **65**, SIAM, 1995.

[16] L.L. Schumaker, *Spline Functions: Basic Theory*, John Wiley and Sons, New York, 1981.